

Intrinsic aggregation propensity of the p63 and p73 TI domains correlates with p53R175H interaction and suggests further significance of aggregation events in the p53 family

Sebastian Kehrlöesser^{*,1,3}, Christian Osterburg¹, Marcel Tuppi¹, Birgit Schäfer¹, Karen Heather Vousden² and Volker Dötsch^{*,1}

The high percentage of p53 missense mutations found in cancer has been attributed to mutant acquired oncogenic gain of functions. Different aspects of these tumour-promoting functions are caused by repression of the transcriptional activity of p53 family members p63 and p73. A subset of frequently occurring p53 mutations results in thermodynamic destabilisation of the DNA-binding domain (DBD) rendering this domain highly unstable. These conformational mutants (such as p53R175H) have been suggested to directly bind to p63 and p73 via a co-aggregation mechanism mediated by their DBDs. Although the DBDs of p63 and p73 are in fact not sufficient for the interaction as shown previously, we demonstrate here that the transactivation inhibitory (TI) domains within the α -isoform-specific C termini of p63 and p73 are essential for binding to p53R175H. Hence, the closed dimeric conformation of inactive TAp63 α that renders the TI domain inaccessible prevents efficient interaction. We further show that binding to p53R175H correlates with an intrinsic aggregation propensity of the tetrameric α -isoforms conferred by an openly accessible TI domain again supporting interaction via a co-aggregation mechanism.

Cell Death and Differentiation (2016) 23, 1952–1960; doi:10.1038/cdd.2016.75; published online 22 July 2016

p53 is the major quality control factor in somatic cells that functions as an integrator of diverse stress signals leading to the cell cycle arrest or apoptosis.¹ Inactivation of the p53 signalling axis constitutes a hallmark of cancer rendering TP53 the most frequently mutated gene in cancer.² The high frequency of missense mutations still resulting in the expression of a full-length protein (mutant p53 (mutp53)) compared with the mere loss of the wild-type protein (wtp53) has been attributed to an oncogenic gain of functions (GOFs) of these mutants.^{3,4} Although mutations can be found for almost any of the 393 residues, a number of hotspot mutations (R175, G245, R248, R249, R273 and R282) cluster within the central DNA-binding domain (DBD).⁵ R248 and R273 are key residues, which make direct contact to the DNA and the major effect of mutations at these sites is abrogation of specific target site binding (DNA contact mutants). The other hotspot mutations only indirectly affect DNA binding by conformationally destabilising the core domain (conformational or structural mutants) leading to partial or global unfolding^{6–8} and potentially the formation of amyloid-like aggregates.^{9–11}

This destabilisation of the anyhow intrinsically unstable p53 DBD has been correlated with the acquired ability to interact

both with the remaining wtp53 as well as with the p53 family members p63 and p73.^{12–15} p63 and p73 are both able to serve as bona fide tumour suppressors,^{16–18} and, moreover, p63 has more recently also been associated with tumour cell migration and metastasis.^{19,20} Hence, mutp53-mediated inhibition of the transcriptional activity of p63 and p73 contributes to the acquired oncogenic functions and increased aggressiveness of the resulting tumours.^{17,19,21–23} Although the dominant-negative effect of mutp53 on the remaining wtp53 can be explained by the formation of mixed tetramers through specific interaction via the oligomerisation domain (OD) as well as co-aggregation processes,²⁴ the mechanism of interaction with the other family members is controversially discussed.^{12–15,20,25–27}

All p53 family members are expressed from at least two different promoters resulting in full-length (transactivation (TA)) or N-terminally truncated (Δ N) variants^{16,28–30} (Figure 1a). Alternative splicing, in addition, gives rise to multiple C-terminal isoforms such as α , β and γ . In contrast to p53, the α -isoforms of p63 and p73 contain two additional domains, the sterile alpha motif (SAM)^{31,32} and the transactivation inhibitory (TI) domain.³³ On the basis of an intricate interdomain interaction network including the TI domain, TAp63 α , unlike all other family

¹Institute of Biophysical Chemistry, Center for Biomolecular Magnetic Resonance and Cluster of Excellence Macromolecular Complexes (CEF), Goethe University Frankfurt, Frankfurt/Main, Germany and ²Cancer Research UK, Beatson Institute, Glasgow G61 1BD, UK

*Corresponding author: V Dötsch or S Kehrlöesser, Institute of Biophysical Chemistry, Centre for Biomolecular Magnetic Resonance and Cluster of Excellence Macromolecular Complexes (CEF), Goethe University Frankfurt, Max-von-Laue-Strasse 9, Frankfurt/Main 60438, Germany. Tel: +49 69 798 29631; Fax: +49 69 798 29632; E-mail: vdoetsch@em.uni-frankfurt.de or sebastian.kehrlöesser@cruk.cam.ac.uk

³Current address: Cancer Research UK, Cambridge Institute, University of Cambridge, Cambridge CB2 0RE, UK.

Abbreviations: AEC, ankyloblepharon, ectodermal dysplasia, clefting; BN-PAGE, blue native polyacrylamide gel electrophoresis; co-IP, co-immunoprecipitation; DBD, DNA-binding domain; EEC, ectrodactyly, ectodermal dysplasia and cleft lip; GOF, gain of function; mutp53, mutant p53; OD, oligomerisation domain; SAM, sterile alpha motif; SEC, size-exclusion chromatography; TA, transactivation; TD, tetramerisation domain; TI, transactivation inhibitory; wtp53, wild-type p53

Received 26.1.16; revised 19.5.16; accepted 24.6.16; Edited by G Melino; published online 22 July 2016

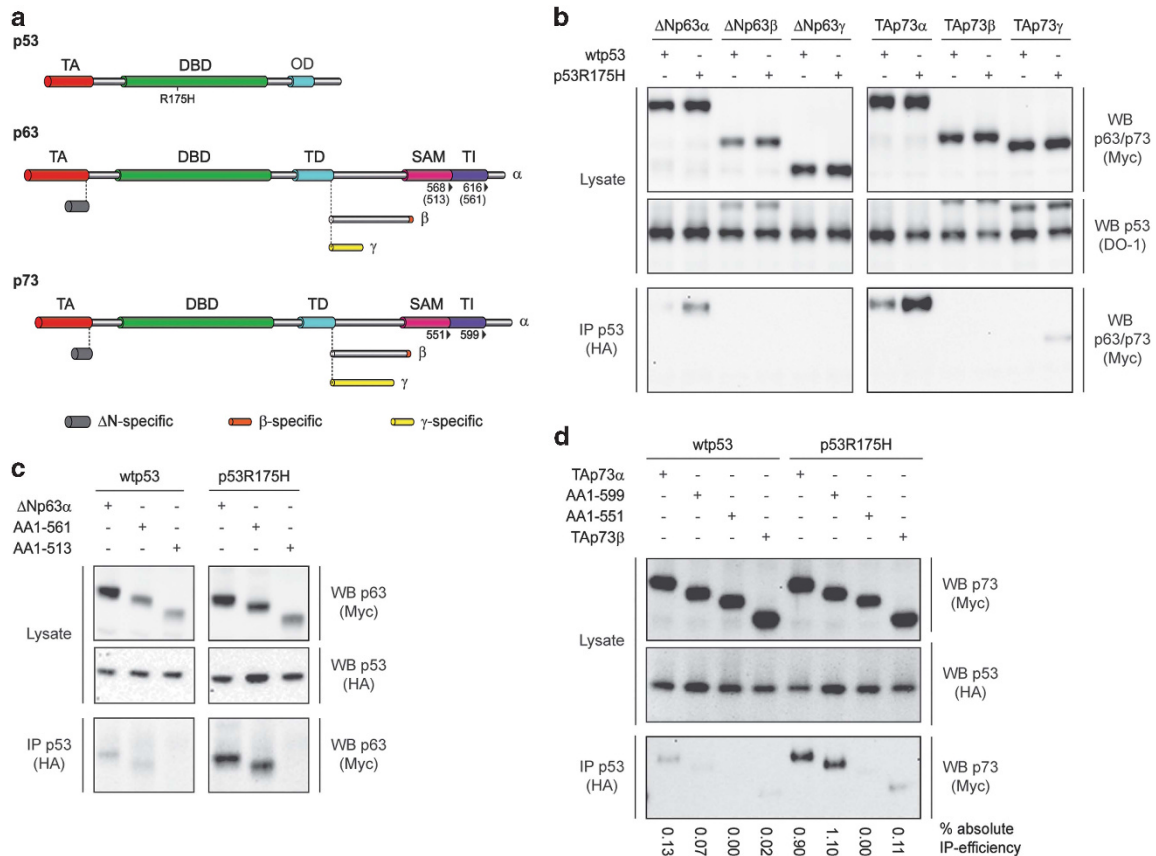


Figure 1 p63 and p73 interact with the conformational p53R175H mutant via their TI domain. (a) The α -isoforms of p63 and p73 contain two additional domains not present in p53, the sterile alpha motif (SAM) and the transactivation inhibitory (TI) domain. Alternative C-terminal splicing results in additional shorter isoforms that contain isoform-specific residues. Limits of truncation constructs used here are indicated by residue numbering based on the respective TA isoform numbering, corresponding Δ Np63 α residue numbers are given in brackets. (b) Various Myc-tagged p63 and p73 isoforms were co-expressed with HA-tagged wild-type (wtp53) or mutant p53 (p53R175H) and co-immunoprecipitated using an HA antibody. C-terminally truncated versions of the α -isoforms of both Δ Np63 α (AA513 and AA561 of Δ Np63 α correspond to AA568 and AA616 in the TAp63 α isoform shown in a) (c) and TAp73 α (d) were used to further define the region required for co-immunoprecipitation (co-IP) with p53R175H. IP efficiencies were determined by densitometric analysis of the IP western blot signals normalised to the input signal strength

members or isoforms, adopts a closed dimeric conformation under unstressed conditions.^{34,35} This conformation reduces the DNA-binding affinity and renders both the TA and TI domain inaccessible.^{35,36}

Although p63 and p73 can heterooligomerise by specific interaction via their tetramerisation domains (TDs), they do not directly interact with the OD of p53.^{37,38} Instead, a previous study suggested that the interaction between mutp53 and p63 or p73 is mediated by the respective DBDs and, moreover, that the unfolding induces exposure of a conserved hydrophobic aggregation motif within the p53 DBD triggering a prion-like co-aggregation with wtp53 as well as with p63 and p73.²⁵

In this study, we systematically re-evaluated the binding of the conformational p53R175H mutant to p63 and p73 as our recent results questioned the essential role of their DBDs.²⁰ In fact, we demonstrate that the TI domains of the α -isoforms confer aggregation propensity and are essential for binding. In addition, assessing the aggregation status of p53R175H in our experimental setting revealed that the majority of this mutant remains folded within cells but readily unfolds under common lysis conditions.

Results

p63 and p73 interact with conformational p53 mutants via their TI domain.

The p53 DBD is thermodynamically the least stable among the p53 family members with a melting temperature slightly above the physiological range.³⁹ Numerous studies could clearly show that further destabilisation by cancer-associated mutations causing partial or complete unfolding of the domain^{8,40} is required to induce interaction with p63 and p73.^{12–15,25} Although the unfolded mutant domain was suggested to induce unfolding and co-aggregation of the remaining metastable wtp53 DBD in a prion-like manner, the significantly higher stability of the p63 and p73 DBDs^{39,41} makes a similar mechanism for the interaction with these family members unlikely. In fact deletion of the DBD of p63 or p73 did not abrogate the interaction with the conformational hotspot mutant p53R175H in our experimental setting.²⁰

Here, we used co-immunoprecipitations (co-IPs) of either wtp53 or p53R175H together with several p63 and p73 isoforms (Figure 1a) or mutants ectopically expressed in Saos-2 cells to map the p63 and p73 regions required for

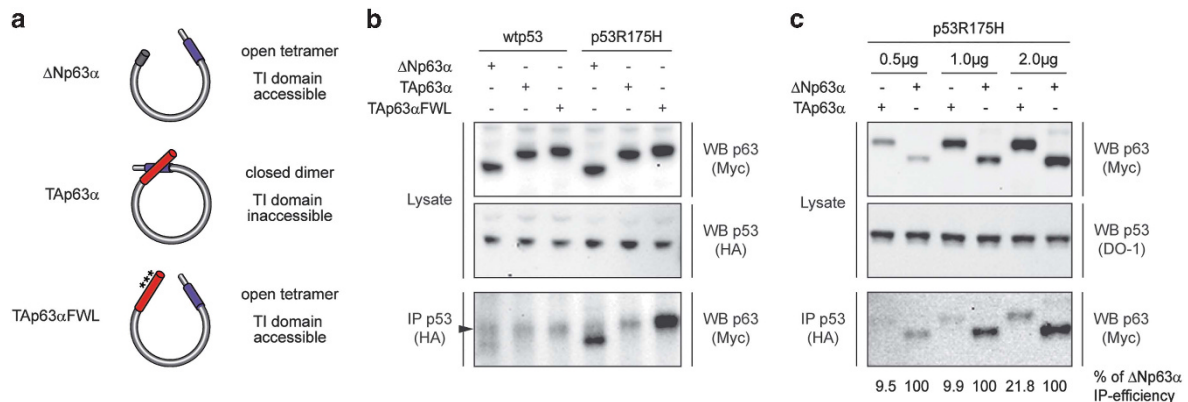


Figure 2 The dimeric conformation of inactive TAp63 α renders the TI domain inaccessible preventing efficient interaction with mutp53. (a) The N-terminal TA domain is involved in the intricate interdomain interaction network required to establish the closed and dimeric conformation of TAp63 α . Absence of the complete N-terminal TA domain in case of Δ Np63 α or mutation of the hydrophobic FWL (F16A, W20A and L23A) motif within the TA domain result in the formation of open tetramers rendering the C-terminal TI domain accessible for intermolecular interactions.³⁵ (b) Co-IP efficiency of the closed dimeric TAp63 α with wtp53 and p53R175H was compared with the tetrameric Δ Np63 α isoform and TAp63 α FWL mutant. Saos-2 cells were co-transfected with 1.0 μ g of the p63 coding plasmids and 1.0 μ g of the wtp53 or p53R175H plasmid. Arrowhead indicates IgG background migrating together with TAp63 α FWL. (c) Cells were transfected with increasing amounts of DNA coding for Δ Np63 α and TAp63 α in combination with p53R175H and IP efficiencies were determined by densitometric analysis of the IP western blot signals normalised to the input signal strength. IP efficiencies for Δ Np63 α were set to 100% for every transfection level

binding to mutp53. In agreement with our latest study,²⁰ these experiments demonstrated that the α -isoforms of Δ Np63 and TAp73 (the isoforms most relevant for suppression of metastasis and tumour development, respectively^{19,42,43}) bind to p53R175H far more strongly than to wtp53, whereas no binding can be observed for any β -isoform or p63 γ (Figure 1b). As previously shown, p73 γ was also able to interact, suggesting that the p73 γ -specific C-terminus reintroduces binding competence.²⁰ As the γ -isoforms of both proteins appear to have minor roles in normal and tumour development, we have focused on the α -C-termini in this study.

The exact interaction motif within the α -C-terminus was further defined using C-terminal truncations of Δ Np63 α (Figure 1c) and TAp73 α (Figure 1d). Removing the entire sequence C-terminal to the SAM domains (Figure 1a) including the TI domain completely abrogated the interaction with mutp53. In contrast, deletion of only the extreme C-termini leaving the TI domains intact⁴⁴ did not influence the binding competence of either protein, suggesting that the TI domain is the essential mediator of the interaction. As the TI domain is unstructured in context of open tetrameric proteins, additional shorter truncations of the p73 TI domain were created (Supplementary Figure 1). Co-IP experiments using these truncated p73 constructs suggested that the C-terminal part of the TI domain is necessary for the interaction, as deletion of only seven amino acids (AA; 593–599) was sufficient to completely abrogate binding.

Dimeric TAp63 α does not interact with p53R175H. In contrast to the open and tetrameric conformation of TAp73 α ,³⁴ TAp63 α adopts a closed and only dimeric state.³⁵ The C-terminal part of the TI domain that is important for the interaction with mutp53 is not accessible in the closed conformation of TAp63 α because it is essential for the intramolecular interactions stabilising the dimeric autoinhibitory conformation (Figure 2a). If the model that only the TI domain but not the DBD interacts with mutp53 is correct, the

dimeric TAp63 α possessing a wild-type DBD but not an openly accessible TI domain should not interact. When we co-expressed p53R175H with TAp63 α in Saos-2 cells, we could not detect significant interaction above background of the dimer with mutp53 (Figure 2b). As a control, we repeated the experiment with Δ Np63 α and the tetrameric TAp63 α FWL mutant (F16A, W20A and L23A),³⁵ which lacks the hydrophobic motif in the TA domain required for dimer formation (Figure 2a). As expected both proteins that have an openly accessible TI domain showed similarly strong co-IPs with mutp53.

According to our model, TAp63 α forms a closed and dimeric conformation without significant transcriptional activity. However, previous studies have observed transcriptional activity as well as binding to mutp53 for TAp63 α .^{15,25} One potential explanation for this discrepancy could be that due to artificially high overexpression levels a minor fraction of TAp63 α adopts an open, tetrameric and active conformation, which is apparent as a smear of higher molecular weight when analysed using blue native polyacrylamide gel electrophoresis (BN-PAGE) (Supplementary Figure 2a). To test this hypothesis, we transfected Saos-2 cells with increasing amounts of a plasmid coding for TAp63 α . In co-IP experiments with mutp53, we could indeed detect an increasing IP signal (Figure 2c; Supplementary Figure 2b), with increasing protein levels. However, the observed co-IP efficiency was always very low compared with tetrameric Δ Np63 α used as a control in the same experiment. This set of experiments suggests that overexpression of TAp63 α results in a small amount of tetrameric TAp63 α that may dominate the result of the experiment.

Transiently expressed p53R175H remains folded inside cells, and the TI domains of p63 and p73 confer self-aggregation propensity to the wild-type proteins. p63 and p73 have been proposed to interact with mutp53 via a co-aggregation mechanism. Hence, we assessed the folding

and aggregation status of p53 and of different isoforms and mutants of p63 and p73 using BN-PAGE (Figure 3) and size-exclusion chromatography (SEC; Supplementary Figures 3a and b). The oligomeric states observed for p53, p63 and p73 (Figure 3) by BN-PAGE correlate well with the kinetic stability of the isolated ODs described previously.^{45,46} p53 showed dimeric and tetrameric fractions, as the overall half-life of the tetramer is the shortest within the p53 family, but the intradimer interface is much more stable than the interdimer interface, which is not the case in p63 and p73. In accordance with the short half-life of the p63 TD (7 min at 37 °C) and the 10 times longer half-life of the p73 TD,⁴⁶ p63 dissociated into dimers and monomers, whereas p73 migrated as tetramers (duration of BN-PAGE ~ 120 min).

Interestingly, when we prepared lysates of transiently transfected Saos-2 cells on ice similar to the sample preparation procedure for the co-IP experiments, p53R175H showed an almost identical migration behaviour compared with the wild-type protein on both BN-PAGE (Figure 3) and SEC (Supplementary Figure 3a). However, when we incubated the samples for 10 min at 37 °C (Supplementary Figure 3a), as used previously in a study analysing the chaperonin-assisted folding of the p53 core domain⁴⁷ or at room temperature for 30 min²⁵ (Figure 3), we observed a marked shift to higher-molecular-weight fractions for p53R175H, whereas wtp53 remained unaffected. wtp53 still readily dissociated into dimers on BN-PAGE and showed no sign of aggregation, whereas p53R175H did no longer dissociate into dimers and displayed a broad migration profile with high apparent molecular weight indicating unfolding of the DBDs (Figure 3). Due to the high local concentration, unfolding of the DBDs first causes formation of aggregate-like structures within a single tetramer²⁴ suppressing the dissociation into lower oligomers. The observation that p53R175H mainly retained a globular overall fold at low temperatures indicates that the majority of this mutant did not unfold inside cells within the timeframe of our experiments. As unfolding is a prerequisite for aggregation and thus potentially the interaction with p63 and p73, this could be an explanation for the low absolute IP efficiency (Figure 1d), as interaction via a co-aggregation mechanism would be expected to result in a neglectable off-rate and thus more efficient interaction.

In agreement with previous observations that the C-terminal part of the p63 TI domain mediates formation of soluble aggregates of purified proteins or peptides,³⁵ BN-PAGE analysis of Δ Np63 α and TAp73 α in comparison with the TI deletion constructs revealed that presence of an accessible TI domain resulted in formation of higher-molecular-weight species in addition to the expected oligomeric states (Figure 3). These results were again supported by SEC experiments of Δ Np63 α in comparison with dimeric TAp63 α (Supplementary Figure 3b). This *ex vivo* aggregation tendency of the TI domain and the unexpected preservation of a globular fold of the p53R175H DBD in a cellular environment prevented further significant demonstration of co-migration with p53R175H due to co-aggregation, as co-expression followed by post-lysis induction of p53 unfolding in the presence of Δ Np63 α was not sufficient to affect the p63 elution profile (Supplementary Figure 3b).

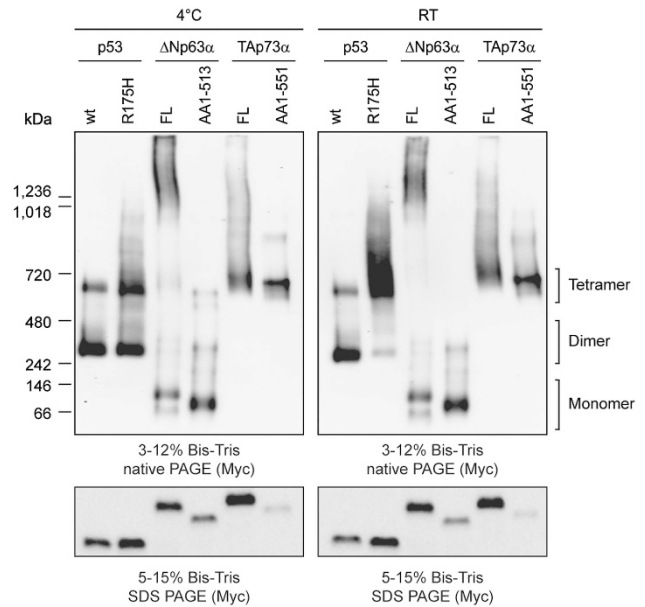


Figure 3 p53R175H remains folded within cells and tetrameric α -isoforms of p63 and p73 are prone to self-aggregate. The oligomeric states and aggregation status of wtp53 and p53R175H as well as Δ Np63 α and TAp73 α and the respective Δ TI constructs (AA513 and AA561 of Δ Np63 α correspond to AA568 and AA616 in the TAp63 α isoform shown in Figure 1a), which were transiently expressed in Saos-2 cells, were assessed by BN-PAGE. Cells were lysed by incubation in BN-PAGE lysis buffer for 30 min on ice (4 °C) or at room temperature (RT). Migration range of the different oligomeric states is indicated by brackets

The p63 TI domain resembles the aggregation inhibitory ReAcP53 peptide. To further characterise the potential role of the TI domain in the proposed co-aggregation with mutp53, we used *in silico* prediction of the β -aggregation propensity. Using the TANGO algorithm,⁴⁸ Xu J *et al.*²⁵ previously identified a highly aggregation prone peptide (amino acids 251–257) within the p53 DBD that could be rendered accessible upon mutation induced unfolding allowing for peptide driven aggregation. When we used this algorithm for the full-length sequences of p53, TAp63 α and TAp73 α at 4 °C corresponding to the experimental conditions in our co-IP experiments, we obtained multiple regions with predicted elevated aggregation propensity (Figures 4a–c; Supplementary Tables 1 and 2). In addition to the previously described conserved β -strand in the DBD (p63 AA282–288 and p73 AA271–277),²⁵ a second β -strand of the DBD and the first α -helix of the SAM domains showed high predicted aggregation propensities (Figures 4b and c; Supplementary Tables 1 and 2). Lower TANGO scores were obtained for the β -strand of the p73 TD, the third helix of the p63 SAM and a region in the TA of p73.

Apart from the low scoring region in the p73 TA domain all sites reside within well-structured regions, do not affect the migration behaviour of the wild-type proteins (Figure 3; Supplementary Figure 3d) and thus should not be accessible for co-aggregation. As expected for a readily accessible sequence, β -aggregation propensity of the C-terminal part of the TI domains was predicted to be <5% (Figure 4d). However, especially the p63 sequence that has a high β -strand propensity and was recently suggested to be part of

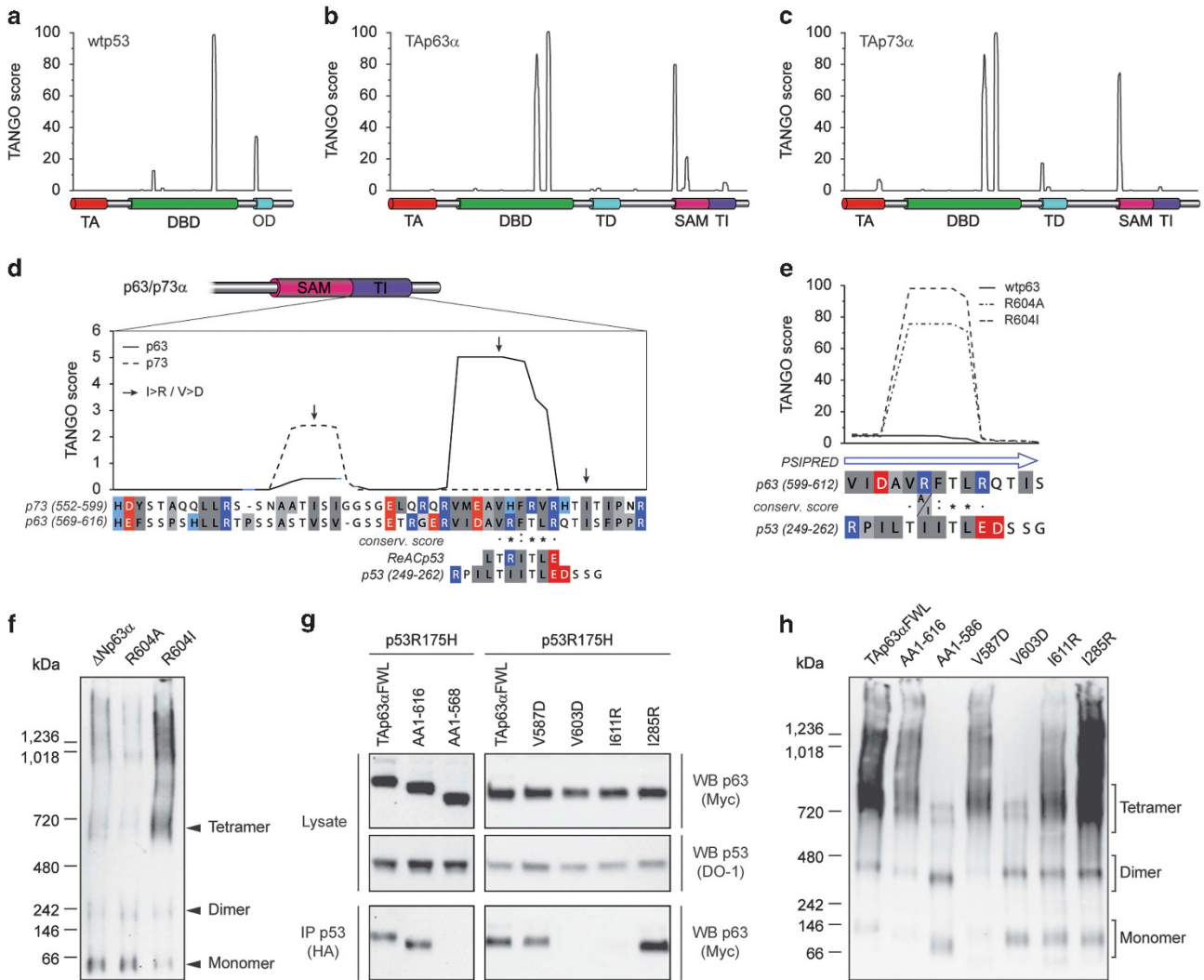


Figure 4 The C-terminal part of the p63 and p73 TI domains structurally resembles the highly aggregation prone p53 DBD motif (AA251–257) and charge introducing mutations prevent self-aggregation and interaction with p53R175H. Primary sequences of wtp53 (a), Tap63 α (b) and Tap73 α (c) were analysed using the TANGO algorithm.⁴⁸ Conditions were set to pH 7.2, ionic strength 0.15 M at a temperature of 4 °C. (d) The C-terminal part of the TI domain shows high-sequence identity with the previously described aggregation inhibitory ReACp53 peptide.⁵⁰ Positions of charge introducing mutations used in co-IP and BN-PAGE experiments are indicated by arrows. The aggregation propensity of mutants rendering the p63 motif more p53 like has been predicted using the TANGO algorithm (e) and experimentally assessed by BN-PAGE (Saos-2 cells) (f). (g) Tap63 α FWL constructs harbouring the TI mutations indicated in (d) were co-expressed with p53R175H in Saos-2 cells for subsequent co-IP experiments. IP efficiencies were compared with the wild-type proteins and the previously published DBD rescue mutation (p63I285R).²⁵ Tap63 α FWL constructs used in g were expressed in H1299 cells and lysates were analysed by BN- and SDS-PAGE followed by subsequent western blotting using a Myc antibody. (h) The self-aggregation of Tap63 α FWL and mutants was analysed by BN-PAGE. Deletion of the TI domain (AA 1–586) or the point mutation V603D completely prevented aggregation, whereas the I285R mutation in the aggregation peptide of the DBD had no effect

an anti-parallel β -sheet in the closed conformation of Tap63 α ⁴⁹ showed high-sequence identity to the recently described ReACp53 peptide (Figure 4d).⁵⁰ This aggregation inhibitory peptide was designed based on a mutation (p53I254R) that was suggested to abolish aggregation of p53R175H and thus interaction with p63 and p73²⁵ (Supplementary Figure 4a). Although the I254R mutation itself induces unfolding of the DBD in context of the full-length protein (Supplementary Figure 4b) and did not abrogate binding to p63 and p73 in our experimental settings,²⁰ potentially by rendering additional aggregation prone regions accessible (Figure 4a), Soragni *et al.*⁵⁰ suggested that the ReACp53 peptide caps growing amyloid steric zipper structures by preventing additional

aggregation prone peptides to anneal. When we exchanged R604 of the p63 TI domain that corresponds to I254R in the alignment shown in Figure 4d with either alanine or isoleucine, the TANGO score was significantly increased to a level observed for the wtp53 peptide (Figure 4e) and substitution to isoleucine in fact promoted the aggregation tendency when analysed by BN-PAGE (Figure 4f).

To further support the hypothesis that the TI domains bind to mutp53, we tested whether replacing hydrophobic amino acids with charged ones at three different sites within the p63 and p73 TI domains (indicated by arrows in Figure 4d) can prevent this interaction. Both C-terminal mutations (V603D and I611R) abrogated binding of Tap63 α FWL (Figure 4g)

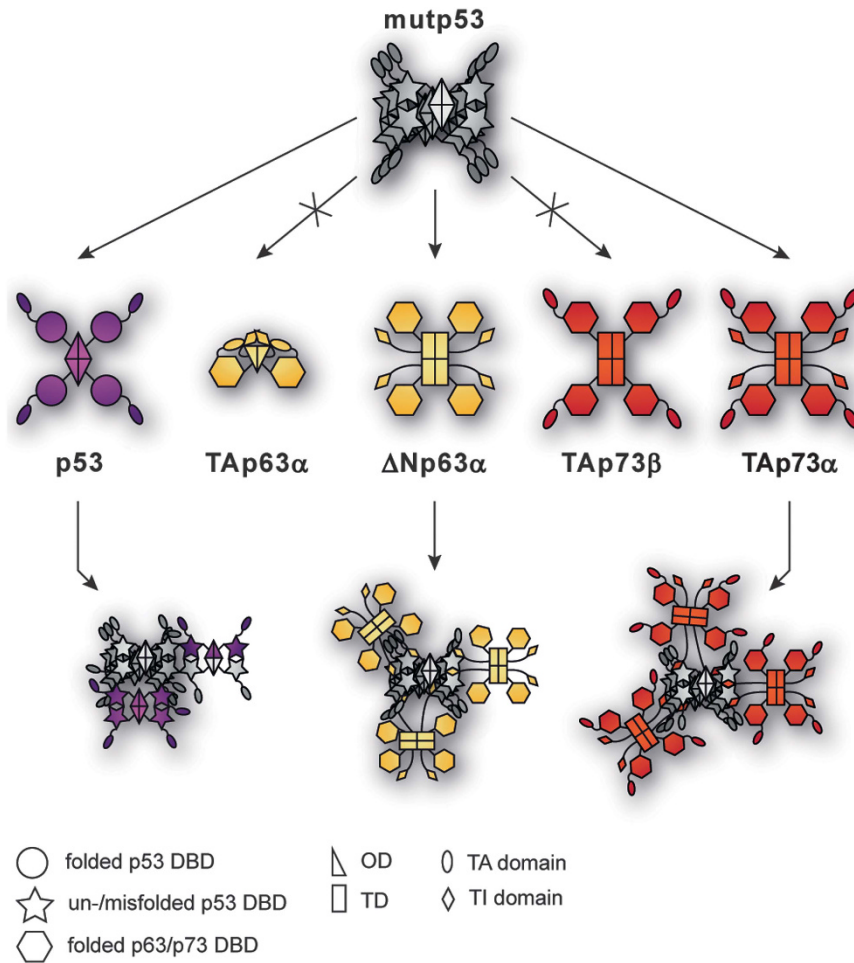


Figure 5 Schematic representation of potential co-aggregation mechanisms of conformational p53 mutants within the p53 family. Mutp53 can interact with remaining wtp53 via specific OD interactions or via the DBD due to induced unfolding. Interaction with p63 and p73, however, is not mediated via the DBD and requires an accessible TI domain

and ΔNp63α (Supplementary Figure 5a) to p53R175H. However, only V603D affected the predicted TANGO score (Supplementary Table 1) and completely prevented self-aggregation of p63 (Figure 4h).

In further support of the essential role of the TI domains, the previously described rescue mutation I285R within the p63 DBD, which was proposed to prevent aggregation with mutp53,²⁵ did not abrogate interaction in our hands (Figure 4h; Supplementary Figure 5a). Furthermore, unlike p53I254R, the homologous mutation within the p63 DBD did not cause the core domain to unfold as it did not significantly affect the populations of the observed oligomeric states (Figure 4h; Supplementary Figure 5d). This observation again demonstrates the increased thermodynamic stability of the p63 DBD that renders amino acids 282–288 within the DBD inaccessible for interaction with mutp53. We have obtained virtually identical results for p73 (Supplementary Figures 5b and c) with one noticeable difference: The p73 TA domain also contains an aggregation promoting peptide (Figure 4c), resulting in the formation of higher-molecular-weight forms when analysed by BN-PAGE even for p73 isoforms lacking the TI domain or having a mutated TI domain containing

additional charged amino acids (Figure 3; Supplementary Figures 3d and 5c).

Discussion

Oncogenic GOFs of cancer-associated hotspot mutations in the p53 gene has partially been correlated with the inactivation of p63 and p73.²¹ Initial co-IP studies as well as a more recent comprehensive co-aggregation analysis pointed to the DBDs of p63 and p73 for mediating the interaction with mutp53.^{13,14,25} The p53 DBD even of the wild-type protein has a low thermodynamic stability with a melting temperature slightly higher than body temperature and is kinetically unstable at physiological temperatures.^{39,51} Hydrophobic and aggregation prone regions that usually reside within the hydrophobic core of the folded domain will become accessible upon unfolding and thus allow for the proposed tetramerisation independent co-aggregation of wtp53 and mutp53 in addition to OD-mediated heterooligomerisation of the wild-type and mutant proteins (Figure 5).

However, our analysis of the aggregation status of wtp53 and the frequently used hotspot mutant p53R175H demonstrated that even the mutant DBD may largely retain an

overall globular fold within cells, rendering the highly aggregation prone motif(s) inaccessible for efficient aggregation. Although this finding correlates well with the limited absolute co-IP efficiency with p63 and p73 in our experiments, this observation raises the question ‘what the exact mechanism of mutp53 promoted aggregation in tumour cells is?’. The low intracellular p53 concentration and its fast turnover rate might prevent aggregation in normal cells. The kinetic behaviour of aggregation is governed by two independent events: initiation and elongation. Typically, the initiation process of forming the first aggregate is the rate-limiting step. Higher intracellular mutp53 concentrations increase the likelihood of some of these molecules forming aggregation nuclei, which will then lead to more efficient self- as well as co-aggregation with other proteins. The required higher intracellular concentration can be triggered by cellular stress signals that typically lead to the increased p53 levels.

Interestingly, although p53R175H may retain a folded core inside cells, standard lysis conditions and downstream analyses caused the mutant domain to unfold, suggesting that evaluation of the folding state of p53 mutants by, for example, reactivity to the conformation-specific PAb240 antibody⁵² may not reflect the actual folding status inside living cells.

In contrast to the proposed co-aggregation mechanism with p63 and p73 requiring the conserved β -strand motif within the core DBD, our data reveal a strict isoform dependence irrespective of the presence of the p63 or p73 DBD (Figure 5). As the DBDs of both p73 and especially p63 exhibit far higher melting temperatures compared with p53,³⁹ these domains are not expected to unfold under physiological conditions. Therefore, co-aggregation mediated by a conserved aggregation motif within the DBD is rather unlikely, as it would be buried within the stable domains. Our detailed mapping of the interaction motif within the α -C termini of p63 and p73 identified the C-terminal part of the TI domain to mediate interaction with p53R175H. Recently, we could show by mutational analysis and theoretical prediction that this region indeed adopts a β -strand configuration as part of the autoinhibitory mechanism that locks TAp63 α in a dimeric inactive state.⁴⁹

In particular, p63 shows a high-sequence identity to the previously published ReACp53 peptide, further supporting that the TI domains of p63 and p73 adopt a β -strand conformation similar to the aggregation motif within the p53 DBD. However, in contrast to the p53 DBD motif, the TI domains of p63 and p73 are readily accessible in tetrameric isoforms. This accessibility of the TI domains confers a certain degree of aggregation tendency to tetrameric α -isoforms of p63 and p73, which can be detected by BN-PAGE or SEC. However, the predicted β -aggregation propensity of the wild-type TI domains is quite low due to the presence of positive charges (p63 R604 and p73 R589) within these motifs (Figure 4f). In particular, Δ Np63 α reaches high expression levels in the basal layer of stratified epithelial tissues,^{28,53} and a high aggregation propensity could lead to aggregation-associated loss of function already at physiological protein levels. Although aggregation is readily detectable *in vitro*, it seems likely that *in vivo* self-aggregation is suppressed by the interaction of the TI domains with other cellular factors.⁵⁴ In the

presence of highly aggregation prone sequences, for example, created by destabilising mutations in the p53 DBD, co-aggregation, however, might occur.

All sequences found in p63 and p73 that show a high aggregation propensity are located in well-structured regions. In principle, mutations within these structured domains could lead to partial or global unfolding resulting in the exposure of these sequences as described for mutp53. In fact, mutations in the p63 DBD or SAM domain result in two related human syndromes, EEC (ectrodactyly, ectodermal dysplasia and cleft lip)⁵⁵ and AEC (ankyloblepharon, ectodermal dysplasia, clefting) syndrome.⁵⁶ Some of the EEC syndrome-associated mutations in the p63 DBD correspond to conformational p53 mutations.⁵⁷ Hence, it would be interesting to see whether these mutations also result in sufficient destabilisation to cause unfolding, especially as introduction of a positive charge within the central β -strand of the DBDs of p53 (I254R) and p63 (I285R) only caused the p53 domain to unfold (Figure 4h; Supplementary Figure 4b). Although this observation suggests that unfolding might not have a role in EEC, it could be the molecular mechanism of missense mutations in the p63 SAM domain found in AEC syndrome patients, as many of these mutations have already been shown to highly destabilise the domain^{58,59} and strikingly also point mutations in the TI domain (R598L and D601V) that increase the aggregation propensity similar to R604I used in this study (Supplementary Table 3) have been associated with this syndrome.⁶⁰

Materials and Methods

Plasmids. Mammalian cell expression constructs for human TAp63 α , Δ Np63 α , TAp73 α and TAp73 β isoforms, and mutants used in this study have been described earlier.^{34,35,44} Δ Np63 β (NM_001114981.1), Δ Np63 γ (NM_001114982.1), Δ Np73 β (NM_001126241.2) and TAp73 γ (NM_001204185.1) were cloned accordingly. HA-tagged wtp53 and p53R175H were a gift from Gerry Melino. Myc-tagged versions of wtp53 and R175H as well as all other mutants were generated employing the Quickchange site-directed mutagenesis protocol.

Cell culture and co-IP. The osteosarcoma cell line Saos-2 was maintained in DMEM containing 10% FBS (Thermo Fisher Scientific, Waltham, USA, MA), 2 mM L-glutamine (Thermo Fisher Scientific) and 1 \times penicillin/streptomycin (Thermo Fisher Scientific) at 37 °C and 5% CO₂. H1299 cells, a non-small cell lung adenocarcinoma cell line, was grown in RPMI 1640, 10% FBS (Thermo Fisher Scientific), 2 mM L-glutamine (Thermo Fisher Scientific) and 1 \times penicillin/streptomycin (Thermo Fisher Scientific) at 37 °C and 5% CO₂. For co-IP assays, Saos-2 cells were co-transfected with HA-tagged wtp53 or p53R175H and different isoforms or mutants of Myc-tagged p63 or p73 using Effectene (Qiagen, Hilden, Germany) according to the manual. Twenty-four hours after transfection, cells were collected and lysed on ice in RIPA cell lysis buffer (Cell Signalling Technology, Danvers, MA, USA) supplemented with 1 mM DTT and protease inhibitor cocktail (Roche, Rotkreuz, Switzerland) for 30 min. Lysates were cleared by centrifugation and the supernatant was incubated with 1 μ g of anti-HA antibody (goat polyclonal, Bethyl Laboratories, Montgomery, TX, USA) overnight at 4 °C. Immunocomplexes were removed from the lysate using Protein G Dynabeads (Thermo Fisher Scientific), washed four times with ice-cold 25 mM Tris (pH 7.8), 250 mM NaCl, 0.1% Tween-20 and eluted with LDS-sample buffer (Thermo Fisher Scientific) supplemented with reducing agent (Thermo Fisher Scientific) for 10 min at 70 °C. Samples were analysed by western blotting. Immunoprecipitation efficiency was calculated by normalisation of the IP western blot signal to the respective input signal.

Western blotting. Western blotting was performed as previously described.⁴⁴ The following antibodies were used: anti-Myc (clone 4A6, Merck Millipore, Darmstadt, Germany), anti-HA (goat polyclonal, Bethyl Laboratories) and anti-p53

(DO-1, Santa Cruz Biotechnologies, Heidelberg, Germany). Quantification of western blot signals was performed using ImageJ (<http://rsb.info.nih.gov/ij/>).

Size-exclusion chromatography. SEC experiments were performed at 4 °C using a Superose 6 PC 3.2/300 column (GE Healthcare, Chalfont St Giles, UK) as previously described³⁵ with an injection volume of 50 µl. Proteins were expressed in Saos-2 cells by transient transfection (Effectene, Qiagen) following the manufacturer's instructions. Fractions were analysed by western blotting.

BN-PAGE. Blue native PAGE gel electrophoresis was performed with NativePAGE Novex 3–12% Bis-Tris protein gels (Thermo Fisher Scientific) according to the manufacturer's instructions, using light blue cathode buffer. Cells were seeded in 12-well plates and transfected using Effectene (Qiagen) according to the manufacturer's protocol. Twenty-four hours after transfection, cells were lysed by incubation on ice or at room temperature for 30 min in 50 µl BN-PAGE lysis buffer (20 mM Tris (pH 7.4), 150 mM NaCl, 2 mM MgCl₂, 1 mM DTT, 20 mM CHAPS supplemented with 1 × protease inhibitor cocktail (Roche) and 0.5 µl benzonase (Merck Millipore) per sample). Separation of 5 µl of the non-cleared lysates supplemented with 2.5 µl 3 × BN-PAGE sample buffer (60% glycerol and 15 mM Coomassie Brilliant Blue G-250) was performed with ice-cold buffers at 4 °C for 60 min at 150 V, followed by 60 min at 250 V. For presentation purposes, blots may have been scaled unidirectionally.

In silico analysis of aggregation propensity. β-Aggregation propensities of wtp53, TAp63α and TAp73α were determined using the TANGO algorithm (<http://tango.crg.es/>; pH 7.2, ionic strength 0.15 M, temperature 4 °C or 37 °C). Due to sequence length restrictions, TAp63α and TAp73α N- and C-terminal part have been predicted separately with large sequence overlaps and results have been merged subsequently.

Conflict of Interest

The authors declare no conflict of interest.

Acknowledgements. The research was funded by the DFG (DO 545/8-1), the Centre for Biomolecular Magnetic Resonance (BMRZ), and the Cluster of Excellence Frankfurt (Macromolecular Complexes).

1. Vousden KH, Lane DP. P53 in health and disease. *Nat Rev Mol Cell Biol* 2007; **8**: 275–283.
2. Muller PA, Vousden KH. p53 mutations in cancer. *Nat Cell Biol* 2013; **15**: 2–8.
3. Brosh R, Rotter V. When mutants gain new powers: news from the mutant p53 field. *Nat Rev Cancer* 2009; **9**: 701–713.
4. Oren M, Rotter V. Mutant p53 gain-of-function in cancer. *Cold Spring Harb Perspect Biol* 2010; **2**: a001107.
5. Freed-Pastor WA, Prives C. Mutant p53: one name, many proteins. *Genes Dev* 2012; **26**: 1268–1286.
6. Joerger AC, Fersht AR. Structure-function-rescue: the diverse nature of common p53 cancer mutants. *Oncogene* 2007; **26**: 2226–2242.
7. Bullock A, Henckel J, DeDecker B, Johnson C, Nikolova P, Proctor M *et al*. Thermodynamic stability of wild-type and mutant p53 core domain. *Proc Natl Acad Sci USA* 1997; **94**: 14338–14342.
8. Ang HC, Joerger AC, Mayer S, Fersht AR. Effects of common cancer mutations on stability and DNA binding of full-length p53 compared with isolated core domains. *J Biol Chem* 2006; **281**: 21934–21941.
9. Levy CB, Stumbo AC, Ano Bom AP, Portari EA, Carneiro Y, Silva JL *et al*. Co-localization of mutant p53 and amyloid-like protein aggregates in breast tumors. *Int J Biochem Cell Biol* 2011; **43**: 60–64.
10. Ano Bom AP, Rangel LP, Costa DCF, de Oliveira GAP, Sanches D, Braga CA *et al*. Mutant p53 aggregates into prion-like amyloid oligomers and fibrils: implications for cancer. *J Biol Chem* 2012; **287**: 28152–28162.
11. Wang G, Fersht AR. Propagation of aggregated p53: cross-reaction and coaggregation vs. seeding. *Proc Natl Acad Sci USA* 2015; **112**: 2443–2448.
12. Di Como CJ, Gaiddon C, Prives C. p73 function is inhibited by tumor-derived p53 mutants in mammalian cells. *Mol Cell Biol* 1999; **19**: 1438–1449.
13. Gaiddon C, Lokshin M, Ahn J, Zhang T. A subset of tumor-derived mutant forms of p53 down-regulate p63 and p73 through a direct interaction with the p53 core domain. *Mol Cell Biol* 2001; **21**: 1874–1887.
14. Strano S, Munarriz E, Rossi M, Cristofanelli B, Shaul Y, Castagnoli L *et al*. Physical and functional interaction between p53 mutants and different isoforms of p73. *J Biol Chem* 2000; **275**: 29503–29512.

15. Strano S, Fontemaggi G, Costanzo A, Rizzo MG, Monti O, Baccarini A *et al*. Physical interaction with human tumor-derived p53 mutants inhibits p63 activities. *J Biol Chem* 2002; **277**: 18817–18826.
16. Kaghad M, Bonnet H, Yang A, Creancier L, Biscan JC, Valent A *et al*. Monoallelically expressed gene related to p53 at 1p36, a region frequently deleted in neuroblastoma and other human cancers. *Cell* 1997; **90**: 809–819.
17. Flores ER, Sengupta S, Miller JB, Newman JJ, Bronson R, Crowley D *et al*. Tumor predisposition in mice mutant for p63 and p73: evidence for broader tumor suppressor functions for the p53 family. *Cancer Cell* 2005; **7**: 363–373.
18. Tan EH, Morton JP, Timpson P, Tucci P, Melino G, Flores ER *et al*. Functions of TAp63 and p53 in restraining the development of metastatic cancer. *Oncogene* 2014; **33**: 3325–3333.
19. Tucci P, Agostini M, Grespi F, Markert EK, Terrinoni A, Vousden KH *et al*. Loss of p63 and its microRNA-205 target results in enhanced cell migration and metastasis in prostate cancer. *Proc Natl Acad Sci USA* 2012; **109**: 15312–15317.
20. Stindt MH, Muller PA, Ludwig RL, Kehrlöesser S, Dötsch V, Vousden KH. Functional interplay between MDM2, p63/p73 and mutant p53. *Oncogene* 2015; **34**: 4300–4310.
21. Li Y, Prives C. Are interactions with p63 and p73 involved in mutant p53 gain of oncogenic function? *Oncogene* 2007; **26**: 2220–2225.
22. Weissmueller S, Manchado E, Saborowski M, Morris JP, Wagenblast E, Davis C. *a et al*. Mutant p53 drives pancreatic cancer metastasis through cell-autonomous PDGF receptor β signaling. *Cell* 2014; **157**: 382–394.
23. Muller PA, Caswell PT, Doyle B, Iwanicki MP, Tan EH, Karim S *et al*. Mutant p53 drives invasion by promoting integrin recycling. *Cell* 2009; **139**: 1327–1341.
24. Lubin DJ, Butler JS, Loh SN. Folding of tetrameric p53: oligomerization and tumorigenic mutations induce misfolding and loss of function. *J Mol Biol* 2010; **395**: 705–716.
25. Xu J, Reumers J, Couceiro JR, De Smet F, Gallardo R, Rudyak S *et al*. Gain of function of mutant p53 by coaggregation with multiple tumor suppressors. *Nat Chem Biol* 2011; **7**: 285–295.
26. Wiech M, Olszewski MB, Tracz-Gaszewska Z, Wawrzynow B, Zyllicz M, Zyllicz A. Molecular mechanism of mutant p53 stabilization: the role of HSP70 and MDM2. *PLoS One* 2012; **7**: e51426.
27. Adorno M, Cordenonsi M, Montagner M, Dupont S, Wong C, Hann B *et al*. A Mutant-p53/Smad complex opposes p63 to empower TGFβ-induced metastasis. *Cell* 2009; **137**: 87–98.
28. Yang A, Kaghad M, Wang Y, Gillett E, Fleming MD, Dötsch V *et al*. p63, a p53 homolog at 3Q27-29, encodes multiple products with transactivating, death-inducing, and dominant-negative activities. *Mol Cell* 1998; **2**: 305–316.
29. Khoury MP, Bourdon J. The isoforms of the p53 protein. *Cold Spring Harb Perspect Biol* 2010; **2**: a000927.
30. Ishimoto O, Kawahara C, Enjo K, Obinata M, Nukiwa T, Ikawa S. Possible oncogenic potential of ΔNp73: A newly identified isoform of human p73. *Cancer Res* 2002; **62**: 636–641.
31. Chi SW, Ayed A, Arrowsmith CH. Solution structure of a conserved C-terminal domain of p73 with structural homology to the SAM domain. *EMBO J* 1999; **18**: 4438–4445.
32. Thanos CD, Bowie JU. p53 family members p63 and p73 are SAM domain-containing proteins. *Protein Sci* 1999; **8**: 1708–1710.
33. Serber Z, Lai HC, Yang A, Ou HD, Sigal MS, Kelly AE *et al*. A C-terminal inhibitory domain controls the activity of p63 by an intramolecular mechanism. *Mol Cell Biol* 2002; **22**: 8601–8611.
34. Luh LM, Kehrlöesser S, Deutsch GB, Gebel J, Coutandin D, Schäfer B *et al*. Analysis of the oligomeric state and transactivation potential of TAp73α. *Cell Death Differ* 2013; **20**: 1008–1016.
35. Deutsch GB, Zelonka EM, Coutandin D, Weber TA, Schäfer B, Hannewald J *et al*. DNA damage in oocytes induces a switch of the quality control factor TAp63α from dimer to tetramer. *Cell* 2011; **144**: 566–576.
36. Suh E-K, Yang A, Kettenbach A, Bamberger C, Michaelis AH, Zhu Z *et al*. p63 protects the female germ line during meiotic arrest. *Nature* 2006; **444**: 624–628.
37. Joerger AC, Rajagopalan S, Natan E, Veprintsev DB, Robinson C V, Fersht AR. Structural evolution of p53, p63, and p73: implication for heterotetramer formation. *Proc Natl Acad Sci USA* 2009; **106**: 17705–17710.
38. Coutandin D, Löhner F, Niesen FH, Ikeya T, Weber TA, Schäfer B *et al*. Conformational stability and activity of p73 require a second helix in the tetramerization domain. *Cell Death Differ* 2009; **16**: 1582–1589.
39. Brandt T, Kaar JL, Fersht AR, Veprintsev DB. Stability of p53 homologs. *PLoS One* 2012; **7**: e47889.
40. Joerger AC, Fersht AR. Structural biology of the tumor suppressor p53 and cancer-associated mutants. *Adv Cancer Res* 2007; **97**: 1–23.
41. Klein C, Georges G, Künkele KP, Huber R, Engh R a., Hansen S. High thermostability and lack of cooperative DNA binding distinguish the p63 core domain from the homologous tumor suppressor p53. *J Biol Chem* 2001; **276**: 37390–37401.
42. Irwin MS, Kondo K, Marin MC, Cheng LS, Hahn WC, Kaelin WG. Chemosensitivity linked to p73 function. *Cancer Cell* 2003; **3**: 403–410.
43. Talos F, Nemajerova A, Flores ER, Petrenko O, Moll UM. p73 suppresses polyploidy and aneuploidy in the absence of functional p53. *Mol Cell* 2007; **27**: 647–659.
44. Straub WE, Weber TA, Schäfer B, Candi E, Durst F, Ou HD *et al*. The C-terminus of p63 contains multiple regulatory elements with different functions. *Cell Death Dis* 2010; **1**: e5.

45. Brandt T, Petrovich M, Joerger AC, Veprintsev DB. Conservation of DNA-binding specificity and oligomerisation properties within the p53 family. *BMC Genomics* 2009; **10**: 628.
46. Natan E, Joerger AC. Structure and kinetic stability of the p63 tetramerization domain. *J Mol Biol* 2012; **415**: 503–513.
47. Trinidad AG, Muller PAJ, Cuellar J, Klejnot M, Nobis M, Valpuesta JM *et al*. Interaction of p53 with the CCT complex promotes protein folding and wild-type p53 activity. *Mol Cell* 2013; **50**: 805–817.
48. Fernandez-Escamilla A-M, Rousseau F, Schymkowitz J, Serrano L. Prediction of sequence-dependent and mutational effects on the aggregation of peptides and proteins. *Nat Biotechnol* 2004; **22**: 1302–1306.
49. Coutandin D, Osterburg C, Srivastav RK, Sumyk M, Kehrlöesser S, Gebel J *et al*. Quality control in oocytes by p63 is based on a spring-loaded activation mechanism on the molecular and cellular level. *Elife* 2016; **5**: e13909.
50. Soragni A, Janzen DM, Johnson LM, Lindgren AG, Thai-Quynh Nguyen A, Tiourin E *et al*. A designed inhibitor of p53 aggregation rescues p53 tumor suppression in ovarian carcinomas. *Cancer Cell* 2015; **29**: 90–103.
51. Khoo KH, Andreeva A, Fersht AR. Adaptive evolution of p53 thermodynamic stability. *J Mol Biol* 2009; **393**: 161–175.
52. Gannon J V, Greaves R, Iggo R, Lane DP. Activating mutations in p53 produce a common conformational effect. A monoclonal antibody specific for the mutant form. *EMBO J* 1990; **9**: 1595–1602.
53. Laurikkala J, Mikkola ML, James M, Tummers M, Mills AA, Thesleff I. p63 regulates multiple signalling pathways required for ectodermal organogenesis and differentiation. *Development* 2006; **133**: 1553–1563.
54. Ramsey MR, He L, Forster N, Ory B, Ellisen LW. Physical association of HDAC1 and HDAC2 with p63 mediates transcriptional repression and tumor maintenance in squamous cell carcinoma. *Cancer Res* 2011; **71**: 4373–4379.
55. Celli J, Duijif P, Hamel BCJ, Bamshad M, Kramer B, Smits APT *et al*. Heterozygous germline mutations in the p53 homolog p63 are the cause of EEC syndrome. *Cell* 1999; **99**: 143–153.
56. McGrath J, Duijif PH, Doetsch V, Irvine A, de Waal R, Vanmolkot KR *et al*. Hay-Wells syndrome is caused by heterozygous missense mutations in the SAM domain of p63. *Hum Mol Genet* 2001; **10**: 221–229.
57. Rinne T, Brunner HG, Van Bokhoven H. p63-associated disorders. *Cell Cycle* 2007; **6**: 262–268.
58. Sathyamurthy A, Freund SM V, Johnson CM, Allen MD, Bycroft M. Structural basis of p63alpha SAM domain mutants involved in AEC syndrome. *FEBS J* 2011; **278**: 2680–2688.
59. Cicero DO, Falconi M, Candi E, Mele S, Cadot B, Di Venere A *et al*. NMR structure of the p63 SAM domain and dynamical properties of G534V and T537P pathological mutants, identified in the AEC syndrome. *Cell Biochem Biophys* 2006; **44**: 475–489.
60. Rinne T, Bolat E, Meijer R, Scheffer H, van Bokhoven H. Spectrum of p63 mutations in a selected patient cohort affected with ankyloblepharon-ectodermal defects-cleft lip/palate syndrome (AEC). *Am J Med Genet A* 2009; **149A**: 1948–1951.

Supplementary Information accompanies this paper on Cell Death and Differentiation website (<http://www.nature.com/cdd>)